Sensitivity of Parameters Employed in Semiempirical Treatment of Displacement Reactions. A Comparison between an Energy-Dependent Hard Model and a Soft Model

Michael Baer* and Saadia Amiel

Contribution from the Nuclear Chemistry Department, Soreq Nuclear Research Centre, Yavne, Israel. *Received July 18, 1970*

Abstract: The recently published energy-dependent hard model for displacement reactions and the soft model due to Karplus and Raff are compared in detail by studying simultaneous trajectories in each of them. The study is performed for different sets of masses and almost over the entire reactive zone (above thermal energies), thus permitting a detailed analysis of the semiempirical parameters used in the two models.

Recently a model[1,2] was presented which permits the computation of the cross sections for energetic displacement reactions of the type

$$ZY + X \longrightarrow ZX + Y \qquad (1)$$

where X and Y are isotopes and Z is an atom or a group of atoms which is assumed to behave as a single particle. The model follows the general lines of the model assumed by Karplus and Raff,[3,4] but the semiempirical Blais–Bunker potential[5,6] used by Karplus and Raff is replaced by a cutoff potential; specifically, the ordinary Morse potentials of the respective particles are replaced by square well potentials and the exponential repulsion term is replaced by a rigid ball potential. This change, which essentially describes an energy-dependent hard model, has permitted a relatively simple treatment of the three interacting particles X, Y, and Z during the reaction process, and served as a check on the sensitivity of the semiempirical parameters used.

The model was tested by comparing the results with those derived by Karplus, Porter, and Sharma[7] for the reaction

$$H_2(D_2) + T \longrightarrow H(D)T + H(D) \qquad (2)$$

The fit was found satisfactory.

The comparison with experiment involves the use of the reaction integral R which is defined as[8]

$$R = \int \frac{\sigma(E)}{E} E \qquad (3)$$

where $\sigma(E)$ is the total reactive cross section and E is the laboratory kinetic energy of the projectile, X, which interacts with the target molecule ZY. The latter is assumed to be stationary. Seewald, Gersh, and Wolfgang[8] determined experimentally the ratio R_{H_2}/R_{D_2} for reaction 2, and Wolfgang and Seewald[9] determined the ratio R_{HT}/R_{DT} for reaction 4. In both

$$HD + T \longrightarrow \begin{cases} HT + D \\ DT + H \end{cases} \qquad (4)$$

cases, the values calculated by the "hard" model[1] were in good agreement with the experimental results.

An extension of the above calculations based on the hard model (henceforward HM) to other cases disclosed disagreements with the values derived from the apparently more realistic soft model (SM) of Karplus and Raff. The deviations appeared mainly in the high-energy region (>10 eV) and at two extremes: (i) when the mass of Z was much greater than the masses of X and Y, and (ii) when the masses of X and Y were much greater than the mass of Z. In the first case the HM-calculated cross sections were too large, and in the second case they were too small.

A comparison between the two models can be performed, since the major difference between them is that different energy surfaces are assumed, but both surfaces, as will be shown, are determined essentially by the same basic parameters and are therefore interrelated. Since the treatments of both the SM and the HM are semiempirical, it was decided to go through a systematic test of the sensitivity of the cross sections calculated by the two models to the parameters used. This may eventually lead to a better insight into the more realistic SM, since the details of the interactions in the HM are relatively simple and well understood, and by adding a few assumptions the HM can be brought rather close to the SM. Furthermore, the importance of the different parameters and terms of the Blais–Bunker potential used in the SM can be deduced.

In the study reported here the two models were compared by performing a series of trajectory calculations and examining the resulting cross sections.

As a final comment we would like to emphasize that this study and the conclusions drawn do not refer to the thermal-energy region, where other studies[3,4,10] strongly support the assumption that the potential governing the interaction between the particles involved is of a soft nature.

The Models

(1) Initial Conditions. In order to perform a systematic comparison between the two models, the initial conditions for each trajectory are taken to be the same:

---

* Address correspondence to this author at the A. A. Noyes Laboratories of Chemical Physics, California Institute of Technology, Pasadena, Calif. 91109.

(1) M. Baer and S. Amiel, *J. Amer. Chem. Soc.*, **91**, 6547 (1969); M. Baer and S. Amiel, *Israel J. Chem.*, 7, 341 (1969).

(2) M. Baer, *J. Chem. Phys.*, **54**, 3670 (1971).

(3) M. Karplus and L. M. Raff, *ibid.*, **41**, 1267 (1964).

(4) L. M. Raff and M. Karplus, *ibid.*, **44**, 1212 (1966).

(5) H. C. Blais and D. L. Bunker, *ibid.*, **37**, 2713 (1962).

(6) H. C. Blais and D. L. Bunker, *ibid.*, **39**, 315 (1963).

(7) M. Karplus, R. N. Porter, and R. D. Sharma, *ibid.*, **45**, 3871 (1966).

(8) D. Seewald, M. Gersh, and R. Wolfgang, *ibid.*, **45**, 3870 (1966).

(9) D. Seewald and R. Wolfgang, *ibid.*, **46**, 1207 (1967).

(10) P. J. Kuntz, M. H. Mok, and J. C. Polanyi, *ibid.*, 50, 4623 (1969).

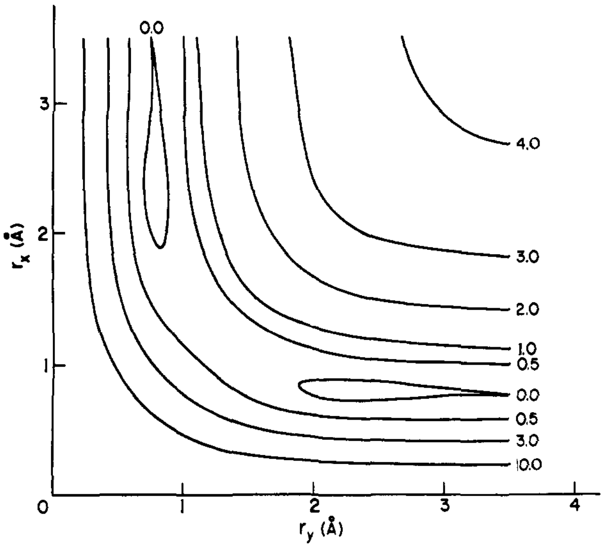

Figure 1. Potential energy surface for linear Y–Z–X, according to SM. Energy contours are in electron volts relative to $V = V_{0x} =$ 4.4 eV for the infinitely separated atoms (R_x = X–Z, R_y = Y–Z in ångströms).

the origin is assumed to be at the center of mass of the system ZY, and the z axis is along the axis of the molecule. The distance between Y and Z at time $t = 0$ is L and the projectile X is at the point **R**. Thus at $t = 0$ the position coordinates of the three particles are

$$Z\left(0,\ 0,\ \frac{m_y}{m_y + m_z}L\right)$$

$$Y\left(0,\ 0,\ -\frac{m_z}{m_y + m_z}L\right) \tag{5}$$

$$X\,(R \sin\theta \cos\phi,\ R \sin\theta \sin\phi,\ R \cos\theta)$$

where R is the distance of X from the center of mass of the ZY system and θ and ϕ are the polar coordinates which determine the direction of **R**.

The initial momenta of Z and Y are taken as zero, whereas for the projectile one finds that for a given initial kinetic energy E the momentum P takes the form

$$P_x = P(\cos\theta \cos\phi \sin\delta \cos\eta - \sin\phi \sin\delta \sin\eta + \sin\theta \cos\phi \cos\delta)$$

$$P_y = P(\cos\theta \sin\phi \sin\delta \cos\eta + \cos\phi \sin\delta \sin\eta + \sin\theta \sin\phi \cos\delta) \tag{6}$$

$$P_z = P(-\sin\theta \cos\eta \sin\delta + \cos\theta \cos\delta)$$

where $P = \sqrt{2m_xE}$ and δ and η are the polar angles determining the direction of the vector **P** in a coordinate system in which z is in the direction of **R**. As can be easily verified, the different trajectories are independent of the angle ϕ, so that ϕ can be assumed to be zero.

(2) The Potential Energy Field. The potential energy fields for the two models can be written in the form

$$V(r_x, r_y, r_{xy}) = V_x(r_x, r_y) + V_y(r_y, r_x) + V_{x,y}(r_x, r_y) + V_{xy}(r_{xy}) \tag{7}$$

where r_x is the distance between Z and X, r_y is the distance between Z and Y, and r_{xy} is the distance between Y and X. In SM, the terms $V_y(r_y, r_x)$ and $V_x(r_x, r_y)$ are the two ordinary Morse potentials, the first for the target molecule ZY and the second for the newly formed molecule ZX.

$$\begin{aligned} V_y(r_y, r_x) &= V_y(r_y) = \\ &V_{0y}(1 - \exp[-\alpha_y(r_y - r_{0y})])^2 - V_{0y} \\ V_x(r_x, r_y) &= V_x(r_x) = \\ &V_{0x}(1 - \exp[-\alpha_x(r_x - r_{0x})])^2 - V_{0x} \end{aligned} \tag{8}$$

In HM these two terms are replaced by square well potentials, *i.e.*

$$V_y(r_y, r_x) = \begin{cases} \infty, \ r_y < \rho_y \text{ for any } r_x \\ -V_{0y}, \ \rho_y \le r_y \le R_y;\ r_x > R_x \\ 0, \ r_y > R_y \text{ for any } r_x \end{cases} \tag{9}$$

and

$$V_x(r_x, r_y) = \begin{cases} \infty, \ r_x < \rho_x; \text{ for any } r_y \\ -V_{0x}, \ \rho_x \le r_x \le R_x;\ r_y > R_y \\ 0, \ r_x > R_x; \text{ for any } r_y \end{cases} \tag{10}$$

In these equations R_y and R_x are the radii of attraction between Z and Y and between Z and X, and ρ_x and ρ_y are the radii of repulsion between Z and Y and Z and X, respectively (see Figure 2). The values of R_x, R_y, ρ_x, and ρ_y are derived from the respective Morse potentials, as will be discussed later.

The potential term $V_{x,y}(r_x, r_y)$ is a three-body potential which reduces the YZ attraction when the X atom is in the vicinity of YZ, and the XZ attraction when Y is in the vicinity of XZ. Thus in SM this term is represented in the form[4]

$$\begin{aligned} V_{x,y}(r_x, r_y) &= \\ &V_{0y}[1 - \tan(\beta_x r_x - \gamma_x)]\exp[-\alpha_y(r_y - r_{0y})] + \\ &V_{0x}[1 - \tan(\beta_y r_y - \gamma_y)]\exp[-\alpha_x(r_x - r_{0x})] \end{aligned} \tag{11}$$

whereas in HM this term takes the form

$$V_{x,y}(r_x, r_y) = \begin{cases} -V_0, \ \rho_x \le r_x \le R_x;\ \rho_y \le r_y \le R_y \\ 0 \text{ elsewhere} \end{cases} \tag{12}$$

The fourth term $V_{xy}(r_{xy})$ stands for the repulsion between X and Y; in SM it takes the exponential form

$$V_{xy}(r_{xy}) = V_{0xy}e^{-\alpha_{xy}(r_{xy} - r_{0xy})} \tag{13}$$

and in HM the hard-sphere form

$$V_{xy}(r_{xy}) = \begin{cases} \infty, \ r_{xy} < \rho_{xy} \\ 0, \ r_{xy} > \rho_{xy} \end{cases} \tag{14}$$

where ρ_{xy} is derived from V_{0xy}, α_x, and r_{0xy}.

The two potential energy surfaces for the linear Y–Z–X system are given in Figures 1 and 2.

(3) Equations of Motion. **(a) The SM Case.** If $\mathbf{q}_x$, $\mathbf{q}_y$, and $\mathbf{q}_z$ are the coordinates of the particles X, Y, and Z in the laboratory system, and $\mathbf{p}_x$, $\mathbf{p}_y$, and $\mathbf{p}_z$ are their momenta, then the generalized coordinates are defined by the relations

$$\begin{aligned} \mathbf{Q}_{zy} &= \mathbf{q}_z - \mathbf{q}_y \\ \mathbf{Q}_{x,yz} &= \mathbf{q}_x - \left(\frac{m_y}{m_y + m_z}\mathbf{q}_y + \frac{m_z}{m_y + m_z}\mathbf{q}_z\right) \\ \mathbf{Q}_{xyz} &= \frac{1}{M}(m_x\mathbf{q}_x + m_y\mathbf{q}_y + m_z\mathbf{q}_z) \end{aligned} \tag{15}$$

where $M = m_x + m_y + m_z$. $\mathbf{Q}_{zy}$ represents the coordinates of Y with respect to Z, $\mathbf{Q}_{x,yz}$ represents the coordinates of X with respect to the center of mass of Y and Z, and $\mathbf{Q}_{xyz}$ represents the coordinates of the center-of-mass system of the three particles. The generalized momenta that are conjugate to the new coordinates are given by the old ones in the form[11]

$$\mathbf{P}_{zy} = \frac{m_y}{m_y + m_z}\mathbf{p}_z - \frac{m_z}{m_y + m_z}\mathbf{p}_y$$

$$\mathbf{P}_{x,yz} = \frac{m_y + m_z}{M}\mathbf{p}_x - \frac{m_y}{M}(\mathbf{p}_z + \mathbf{p}_y) \qquad (16)$$

$$\mathbf{P}_{xyz} = \mathbf{p}_x + \mathbf{p}_y + \mathbf{p}_z$$

Consequently, the Hamiltonian function takes the form

$$H = \frac{1}{2\mu_{yz}}|\mathbf{P}_{zy}|^2 + \frac{1}{2\mu_{x,yz}}|\mathbf{P}_{x,yz}|^2 + \frac{1}{2M}|\mathbf{P}_{xyz}|^2 + V(r_x, r_y, r_{xy}) \qquad (17)$$

where

$$\frac{1}{\mu_{yz}} = \frac{1}{m_y} + \frac{1}{m_z} \qquad \frac{1}{\mu_{x,yz}} = \frac{1}{m_x} + \frac{1}{m_y + m_z}$$

and $V(r_x, r_y, r_{xy})$ is the potential field of which r_x, r_y, and r_{xv} are given in the form

$$r_y = |\mathbf{Q}_{zy}|$$

$$r_x = \left|\frac{m_y}{m_y + m_z}\mathbf{Q}_{zy} - \mathbf{Q}_{x,yz}\right| \qquad (18)$$

$$r_{xy} = \left|\frac{m_z}{m_y + m_z}\mathbf{Q}_{zy} + \mathbf{Q}_{x,yz}\right|$$

Hamilton's equations of motion for the three-body system are given by

$$\frac{dQ_j}{dt} = \frac{\partial H}{\partial P_j}; \quad \frac{dP_j}{dt} = -\frac{\partial H}{\partial \mathbf{q}_j} \qquad (19)$$

where j is an index which signifies the components of the different coordinates and momenta.

These equations can be represented explicitly and are solved numerically by the Runge–Kutta–Gill method.[12] The solution yields the trajectory of the three particles as a function of time.

(b) The HM Case. If $\mathbf{q}_x$, $\mathbf{q}_y$, and $\mathbf{q}_z$ are the coordinates of the particles X, Y, and Z in the laboratory system, and $\mathbf{v}_x$, $\mathbf{v}_y$, and $\mathbf{v}_z$ are their velocities, then the relative coordinates and velocities are as follows

$$\mathbf{r}_{xz} = \mathbf{q}_x - \mathbf{q}_z$$
$$\mathbf{r}_{yz} = \mathbf{q}_y - \mathbf{q}_z \qquad (20)$$
$$\mathbf{r}_{xy} = \mathbf{q}_x - \mathbf{q}_z$$

and

$$\mathbf{v}_{xz} = \mathbf{v}_x - \mathbf{v}_z$$
$$\mathbf{v}_{yz} = \mathbf{v}_y - \mathbf{v}_z \qquad (21)$$
$$\mathbf{v}_{xy} = \mathbf{v}_x - \mathbf{v}_y$$

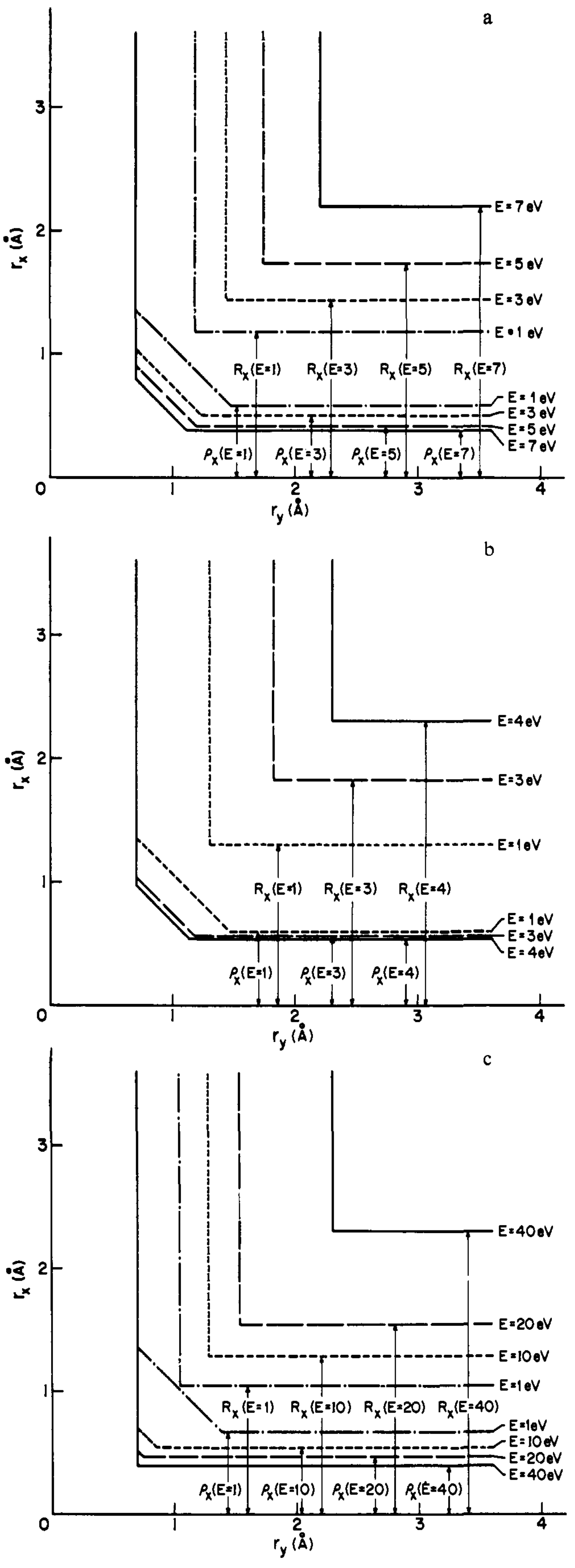

Figure 2. Potential energy surfaces for linear Y-Z-X, according to HM. Contours representing the edges of the different potential regions as a function of the energy E of the projectile (atom X): (a) the surface for the masses $m_x = m_y = m_z = 1$ mu, (b) the surface for the masses $m_x = m_y = 1$ mu, $m_z = 10$ mu; (c) the surface for the masses $m_x = m_y = 10$ mu, $m_z = 1$ mu.

---

(11) E. T. Whittaker, "A Treatise on the Analytical Dynamics of Particles and Rigid Bodies," 4th ed, Cambridge University Press, Cambridge, England, 1937.

(12) S. Gill, *Proc. Cambridge Phil. Soc.*, 47, 96 (1951).

Considering again the representation of the potential energy field, one finds that the interaction between the three particles is, in fact, composed of a series of two-body interactions, where each such interaction is independent of the existence of the third particle. However, since a three-particle system is considered, one has to find which pair of particles is going to collide first. Thus, assuming, for instance, that the last collision took place between X and Y, one has to compute the times t_{yz} and t_{xz}, where t_{yz} is the time that elapses before a collision between Y and Z and t_{xz} is the time that elapses before a collision between X and Z. Consequently if $t_{xz} > t_{yz}$, then Y and Z are going to collide before X and Z do, and the contrary happens if $t_{xz} < t_{yz}$.

If $\mathbf{r}_{yzi}$ is the relative position of Y with respect to Z immediately after the collision between X and Y, then t_{yz} is given by the equation

$$t_{yz} = \frac{1}{\mathbf{v}_{yz}{}^2}\Big[-(\mathbf{v}_{yz}\cdot\mathbf{r}_{yzi}) + \sqrt{(\mathbf{v}_{yz}\cdot\mathbf{r}_{yzi})^2 - |\mathbf{v}_{yz}|^2(|\mathbf{r}_{yzi}|^2 - |\mathbf{r}_{yzf}|^2)}\Big] \tag{22}$$

where $\mathbf{v}_{yz}$ is the relative velocity of Y with respect to Z, and $|\mathbf{r}_{yzf}|^2$ is the distance between Z and Y at the point of contact; *i.e.*, $\mathbf{r}_{yzf}$ equals either R_y or ρ_y (see eq 9). A similar equation exists for t_{xz}. In general, $\mathbf{r}_{yzf}$ is equal to R_y and is only equal to ρ_y if the reduced particle Y–Z hits the inner part of the potential. The conditions for this are

$$(\mathbf{v}_{yz}\cdot\mathbf{r}_{yzi}) < 0 \tag{23}$$

$$\rho_y{}^2 > \left[|\mathbf{r}_{yzi}|^2 - \frac{(\mathbf{v}_{yz}\cdot\mathbf{r}_{yzi})^2}{|\mathbf{v}_{yz}|^2}\right] \tag{24}$$

Similar conditions have to be checked for the reduced particle X–Z.

Assuming, for instance, that the conditions (23) and (24) are fulfilled, and that $t_{xz} > t_{yz}$, one first computes the relative positions of the three particles after time $t = t_{yz}$, *i.e.*

$$\begin{aligned} \mathbf{r}_{xzf} &= \mathbf{r}_{xzi} + t_{yz}\mathbf{v}_{xzi} \\ \mathbf{r}_{yzf} &= \mathbf{r}_{yzi} + t_{yz}\mathbf{v}_{yzi} \\ \mathbf{r}_{xyf} &= \mathbf{r}_{xzf} - \mathbf{r}_{yzf} \end{aligned} \tag{25}$$

One then computes the relative velocities that have changed due to the collision of Y with Z

$$\mathbf{v}_{yzf} = \mathbf{v}_{yzi} - \frac{2}{|\mathbf{r}_{yzf}|^2}(\mathbf{v}_{yzi}\cdot\mathbf{r}_{yzf})\mathbf{r}_{yzf}$$

$$\mathbf{v}_{xzf} = \mathbf{v}_{xzi} - \frac{2}{|\mathbf{r}_{yzf}|^2}\frac{m_y}{m_y + m_z}(\mathbf{v}_{yzi}\cdot\mathbf{r}_{yzf})\mathbf{r}_{yzf}$$

$$\mathbf{v}_{xyf} = \mathbf{v}_{xzf} - \mathbf{v}_{yzf}$$

All the other cases are treated in the same manner.

(4) Tests for the Final State. Considering the system (ZY, X) one would in general expect four possibilities.

$$\mathrm{ZY + X \longrightarrow ZX + Y} \tag{i}$$

$$\mathrm{ZY + X \longrightarrow ZY + X} \tag{ii}$$

$$\mathrm{ZY + X \longrightarrow Z + X + Y} \tag{iii}$$

$$\mathrm{ZY + X \longrightarrow YX + Z} \tag{\textit{iv}}$$

It is easily seen that using the above potential fields, the fourth reaction is excluded, since no attraction is assumed to exist between Y and X. In the case of SM the decision between the three other cases is made by testing the distances between the three particles after an "infinite" time. Thus if the distance between X and Z is finite, then the molecule ZX is formed (case i). If the distance between Y and Z is finite, then no reaction has occurred (case ii). If both distances are infinite, then case iii is met. (The potential field is constructed in such a way that no activated complex can be formed.) Thus one gets the final result in a "natural way" in the sense that one has only to check, after an infinite time, the relative distances between the three particles.

In the case of HM the test is done in the following way. Assuming X to be already in the region of attraction of Z, we follow the motion of the three particles and check which of the two particles X or Y first reaches its boundary of attraction with Z. If, for instance, Y does so, then, according to the assumptions of HM, it leaves Z without causing any changes or disturbances in the system, and the condition for having either (i) or (iii) is dependent on whether the internal energy E_{ix} of the system Z–X is smaller or larger than $V_{0x}/\cos^2\psi_x$, where ψ_x is the angle of collision, *i.e.*, the angle between the trajectory of the reduced particle XZ and the radius of the square well.

The case where X first reaches its boundary of attraction with Z is treated similarly, and the condition of having either (ii) or (iii) is dependent on whether the internal energy E_{iy} of the system Z–Y is smaller or larger than $V_{0y}/\cos^2\psi_y$, where ψ_y is defined in a similar way to ψ_x.

The Comparison between SM and HM. In order to perform a numerical comparison between SM and HM, the following arbitrary values were taken:[13] $V_{0x} = V_{0y} = 4.4$ eV, $V_{0xy} = 0.2$ eV, $r_{0x} = r_{0y} = 0.75$ Å, $\alpha_x = \alpha_y = 1.8$ Å^{-1}, $\beta_x = \beta_y = 1.1$ Å, $\gamma_x = \gamma_y = -0.734$, $r_{0xy} = 2.3$ Å, and $\alpha_{xy} = 3.6$ Å^{-1}.

This group of parameters can be divided into three subgroups. The first includes V_{0x}, V_{0y}, r_{0x} r_{0y}, α_x, and α_y, which are the characteristic parameters of the Morse potentials of ZX and ZY; the second includes the parameters β_x, β_y, γ_x, and γ_y, which appear in the attenuation terms and are determined in such a way as to yield a surface as smooth as possible along the reaction coordinate (as long as the exponential repulsion term is ignored), without dips and bumps[14] (see Figure 1); the third includes the parameters V_{0xy}, r_{0xy}, and α_{xy}, which appear in the exponential repulsion term representing the interaction between X and Y.

These parameters are used to represent the energy potential surface in SM. The first and third subgroups will also be used to derive the energy surface in HM, but the second subgroup will be replaced in HM by only one parameter, *viz.*, V_0, which represents the two attenuation terms in SM. The value of V_0 is assumed to be equal to that of V_{0x} (and V_{0y}).

Although it seems that in order to describe the surface in HM additional parameters have to be introduced, namely R_x, R_y, ρ_x, ρ_y, and ρ_{xy} (those which determine the radius of influence of the different cutoff potentials),

---

(13) The numerical values taken for the different parameters are arbitrary, albeit closely related to the cases treated in ref 1.

(14) In ref 1 it was shown that one can determine the threshold energy for a given reaction using only one term, $V_{xy}(r_{xy})$, of the entire potential; therefore, as long as this term is not included in the potential there is no reason to assume the existence of any bumps or dips in the remaining part of the potential. Using this assumption β_x, β_y, γ_x, and ρ_y were fitted.

it will be shown in the following section that they are closely related to those used in SM.

As has already been mentioned, the results derived by the use of HM (see ref 1) are sometimes in agreement with those obtained from SM and sometimes in disagreement. One of the main factors influencing the correspondence between the two models is the masses of the interacting particles. Therefore, the comparison was made for three extreme cases: the first where the three masses, namely m_x, m_y, and m_z, are equal; the second where the masses m_x and m_y are much greater than m_z; and the third where the mass m_z is much greater than m_x and m_y. The following numerical values were assumed: for the first case, $m_x = m_y = m_z = 1$ mu; for the second, $m_x = m_y = 10$ mu and $m_z = 1$ mu; and for the third, $m_x = m_y = 1$ mu and $m_z = 10$ mu.

In order to get a fit between the two models for the whole range of masses and energies, some of the parameters of HM had to be made energy dependent. First, only ρ_{xy} and ρ_x were made energy dependent,[1] but the fit obtained was limited to certain masses and energies. In order to extend the fit to the most general case, an energy dependence was introduced into the parameters R_x and R_y and the position of Y relative to Z and X at time $t = 0$. In what follows we shall describe how this dependence was derived.

(a) The Dependence of ρ_{xy} on the Energy. Both in the SM and in the HM, the reaction takes place following a direct repulsion between X and Y. It has already been shown in ref 1 that in order to get the correct dependence of the total reactive cross section with respect to the energy, one has to make the total geometric cross section for the collision between X and Y energy dependent, in such a way that the higher the energy of the reduced particle X–Y the smaller the corresponding cross section for collision. The physical justification for this dependence is closely related to the fact that the higher the energy of the reduced particle, the smaller will be the "effective" geometrical cross section for collision which might lead to reaction.

If the potential between X and Y is assumed to be V_{xy} (r_{xy}), then there exist two straightforward ways to define an energy-dependent radius for the analogous billiard ball potential. If b is the impact parameter for the given interaction, then one possibility is to define the radius as the zero of the equation

$$1 - \frac{V_{xy}(r_{xy})}{E_{xy}} - \frac{b^2}{{r_{xy}}^2}\bigg|_{r_{xy}=\rho_{xy}} = 0 \qquad (26a)$$

where E_{xy} is the kinetic energy of the reduced particle X–Y and $V_{xy}(r_{xy})$ is given in (13). The zero of this equation is the closest approach between the two particles X and Y for a given impact parameter b. It turns out that in the low-energy region the values of ρ_{xy} derived in this way yield a good fit between HM and SM. However, in the high-energy region, these ρ_{xy} values give reaction cross sections which are too high, and one has to extract the values of ρ_{xy} from the simpler equation used in ref 1.

$$1 - \frac{V_{xy}(r_{xy})}{E_{xy}}\bigg|_{r_{xy}=\rho_{xy}} = 0 \qquad (26b)$$

The values of ρ_{xy} derived from (26b) are the closest approach of X and Y in a head-on collision, and are relatively smaller than those obtained from (26a).

The relevance of the eq 26a and 26b to the different energy regions, *i.e.*, the "low" and the "high" energy region, is discussed below.

(b) The Dependence of ρ_x on the Energy. The dependence of ρ_x on the energy is the same as was found in ref 1, namely ρ_x is the zero of the equation

$$V_x(r_x) + V_{0x} - E_{xz}|_{r_x=\rho_x} = 0 \qquad (27)$$

where E_{xz} is the initial energy of the reduced particle X–Z.

(c) The Dependence of R_x and R_y on the Energy. In ref 1 it was shown that one can choose the values of R_x and R_y in such a way as to get the correct cross sections without making them energy dependent. The values attached to R_x and R_y were rather small (1 Å each), and the fit derived was satisfactory. However, it turns out that using small radii of attraction in general yields satisfactory results only in the low-energy region, whereas in the high-energy region (>10 eV) the results derived are in certain cases overestimated. This deviation becomes more and more pronounced as the mass of Z becomes greater relative to the masses of X and Y. The reason for this is that when X interacts while possessing high kinetic energy, then the newly formed molecule ZX is highly excited. Since the Morse potential is a rather soft potential, the total internal energy of a diatomic molecule will only rarely exceed the value of the binding energy without dissociating. In sharp contrast to the Morse potential, the square well potential might in certain cases allow the accumulation of an indefinite amount of internal energy in the rotational mode. This is due to the fact that the square well potential is concerned only with the vibrational component of the energy and cannot allow bond stretching (and, hence, rupture) by the centrifugal force of the rotation. It can be shown that the division of energy between vibration and rotation is dependent on the radius of the square well in such a way that the smaller the radius the larger will be the amount of energy stored in the rotational mode ($E_{\text{rot}} \propto (b/r)^2$, $E_{\text{vib}} \propto 1 - (b/r)^2$, where b is the impact parameter). Therefore, if use is made of square well potentials with small radii of attraction, one should expect larger total reactive cross sections (in the high-energy range) than would be expected from using square wells with large radii of attraction.

To summarize this point, we note that in order to get a satisfactory fit along the whole energy range for all the cases under consideration, we have to use potential wells with relatively small radii in the low-energy region and with relatively large radii in the high-energy region. For this purpose, we assume the radii of attraction R_x and R_y to be energy dependent. The dependence is derived in the following way. If E_x is the maximum energy that the atom X can have after the collision with Y, then R_x is determined from the equation

$$V_x(r_x) + V_{0x} - \frac{m_z}{m_x + m_z}E_x\bigg|_{r_x=R_x} = 0 \qquad (28)$$

The energy E_x is in fact equal to the initial energy of X, *viz.*, E, and $V_x(r_x)$ is given in (8). In the same manner R_y is extracted from the equation

$$V_y(r_y) + V_{0y} - \frac{m_z}{m_y + m_z} E_y \big|_{r = R_y} = 0 \tag{29}$$

where $V_y(r_y)$ is given in (8) and E_y is the maximum energy that Y can have following the collision with X, which is

$$E_y = 4\frac{m_x m_y}{(m_x + m_y)^2} E \tag{30}$$

Although we used $V_x(r_x)$ and $V_y(r_y)$ as given in (8), we could not get a satisfactory fit as long as we used the same values for r_{0x} and r_{0y} as are used in SM. These values were therefore changed and serve as parameters which are independent of the energy of the projectile and of the interacting masses. However, since X and Y are isotopes, we assumed $r_{0x} = r_{0y}$. The numerical value for r_{0x} used in HM is 0.95 Å, in contrast to the value of 0.75 Å used in SM.

Equations 28 and 29 are valid as long as E, the initial energy of X, satisfies the two inequalities

$$E < \frac{m_z + m_x}{m_z} V_{0x} \tag{31}$$

and

$$E < \frac{m_z + m_y}{m_z} \frac{(m_x + m_y)^2}{4 m_x m_y} V_{0y} \tag{32}$$

For energies which do not fulfill either of the inequalities 31 or 32, the meaning of the radius of attraction is lost. Thus, in the event that neither of the above inequalities is valid, arbitrary large values were chosen for R_x and R_y (5 Å in the example given below).

The energy E for which one of the above inequalities first becomes an equality will be termed E_{lh}. Thus E_{lh} is defined as

$$E_{lh} = \min\left(\frac{m_z + m_y}{m_z} V_{0x}, \frac{m_z + m_y}{m_z} \frac{(m_x + m_y)^2}{4 m_x m_y} V_{0y}\right) \tag{33}$$

This definition of E_{lh} enables us to divide the whole reactive zone into two parts: the first (0, E_{lh}) will be termed the "low-energy region" and the second (E_{lh}, ∞) the "high-energy region." Returning to the problem of determining ρ_{xy}, eq 26a is used as long a s $E < E_{lh}$ and eq 26b is used when $E > E_{lh}$.

(d) Relative Position Adjustments of X, Y, and Z at Time $t = 0$. In contrast to a hard-sphere interaction between two particles, a soft interaction is a process which takes some finite time. If the interaction occurs between two particles where one is moving (projectile) and the other is initially static (target), then the position of the static particle changes during the course of the interaction. If t_c is the time that elapses from the moment the two particles are a distance R apart until the moment their separation becomes smallest, then in the case of a head-on collision t_c is given in the form[15]

$$t_c = \int_{r_0}^{R} \frac{\mathrm{d}r}{\sqrt{\frac{2E}{\mu}\left(1 - \frac{V(\mathrm{r})}{E}\right)}} \tag{34}$$

where E is the energy at the center of mass of the two particles, μ is the reduced mass, $V(\mathrm{r})$ is the interaction potential, r_0 is the closest approach of the two particles, and R is some arbitrary large distance between the two particles for which one can assume that $V(\mathrm{r}) \sim 0$. The time t_c will be computed for two cases, the first (i)

$$V(r) = Ae^{-\alpha r} \tag{35}$$

In this case we obtain

$$t_c = t_{SM} = \frac{1}{\alpha}\frac{\mu}{2E} \ln\left(\frac{1 + \sqrt{1 - e^{-\alpha(R - r_0)}}}{1 - \sqrt{1 - e^{-\alpha(R - r_0)}}}\right) \tag{36}$$

where, if values of R are large enough, it can be easily shown that

$$t_{SM} = \sqrt{\frac{\mu}{2E}}\left[(R - r_0) + \frac{\ln 4}{\alpha}\right] \tag{37}$$

For the second case (ii)

$$V(\mathrm{r}) = \begin{cases} \infty \text{ for } r < r_0 \\ 0 \text{ for } r > r_0 \end{cases} \tag{38}$$

In this case, one obtains

$$t_c = t_{HM} = \sqrt{\frac{\mu}{2E}}(R - r_0) \tag{39}$$

From eq 37 and 39, we notice that the difference between t_{SM} and t_{HM} is a value independent of R, namely

$$t_{SM} = t_{HM} = \sqrt{\frac{\mu}{2E}}\left(\frac{\ln 4}{\alpha}\right) \tag{40}$$

Consequently, from this point of view, in order to simulate the soft collision, one has to move the target atom away from its original position to such a distance that the time that elapses until the two particles are at their closest is equal in both models. This will happen if the distance in the HM case is increased by an amount $v(t_{SM} - t_{HM})$, where v is the relative velocity, *i.e.*, $v = (2E/\mu)$. Therefore, the change has to be

$$v(t_{SM} - t_{HM}) = \frac{\ln 4}{\alpha} \tag{41}$$

Thus if $\mathbf{r}_{xyi}$ is the relative position of X and Y in SM, then the relative position of the two particles in HM should be

$$\left(|\mathbf{r}_{xyi}| + \frac{\ln 4}{\alpha}\right)\frac{\mathbf{r}_{xyi}}{|\mathbf{r}_{xyi}|}$$

In the same manner, if the relative position of Y and Z in SM is $\mathbf{r}_{yzi}$, then their relative position in HM should be

$$\mathbf{r}_{yzi} + \frac{\ln 4}{\alpha}\frac{\mathbf{r}_{xyi}}{|\mathbf{r}_{xyi}|}$$

These shifts are valid as long as the radius of the well of Z and Y is large enough. However, it may happen (especially at low energies) that such a shift will bring atom Y outside the well. In such a case atom Y is shifted, at most, to a distance such that the separation between Y and Z will not become larger than the radius of the well.

In principle, a similar change in the position of Z has to be made. However, since the main interaction, when X approaches the molecule ZY, is between X and Y, the change in the position of Z can be ignored.

---

(15) L. D. Landau and E. M. Lifshitz, "Mechanics," Pergamon Press, Elmsford, N. Y., 1960.

Results

The comparison between SM and HM was, as mentioned earlier, performed for three sets of masses. In Tables, I, II, and III are presented the total reactive cross sections as a function of the energy of the projectile (atom X) in the laboratory system, for both SM and HM. We can distinguish between two cases: (i) when the angle θ changes from 0 to 180° (if **R** is the initial position of X with respect to the molecule ZY, then θ is the angle between **R** and the axis of the molecule ZY); (ii) when the angle θ changes from 0 to 90°.

Table I. Comparison between the Results of SM and HM for the Masses $m_x = m_y = 10$ mu, $m_z = 1$ mu

	Reactive cross sections, Å^2				
	$0 \leq \theta \leq \pi$		$0 \leq \theta \leq \pi/2$		Percent-
E, eV	SM	HM	SM	HM	age[a]
1	0.05		0.05		
3	0.94	1.15	0.94	1.15	95
5	1.38	1.55	1.38	1.55	94
10	2.35	2.24	2.16	2.02	84
20	2.30	1.82	1.72	1.38	70
40	1.62	1.10	0.98	0.82	52
100	0.92	0.97	0.27	0.30	70

[a] The "fertile" initial conditions (those for which the trajectories end in reactions) are not necessarily the same in the two models. This column shows the percentage of initial conditions which happens to be fertile in both models, expressed as a percentage of the total number of fertile trajectories in SM ($0 \leq \theta \leq \pi/2$).

Table II. Comparison between the Results of SM and HM for the Masses $m_x = m_y = m_z = 1$ mu

	Reactive cross sections, Å^2				
	$0 \leq \theta \leq \pi$		$0 \leq \theta \leq \pi/2$		Percent-
E, eV[a]	SM	HM	SM	HM	age[a]
1	0.58	0.45	0.58	0.45	75
3	2.48	2.35	2.20	2.20	96
5	2.70	2.72	2.10	2.10	98
7	2.86	2.96	1.96	1.91	91
10	2.20	2.34	1.42	1.20	76
15	1.29	1.90	0.67	0.89	83

[a] See footnote a, Table I.

Table III. Comparison between the Results of SM and HM for the Masses $m_x = m_y = 1$ mu, $m_z = 10$ mu

	Reactive cross sections, Å^2				
	$0 \leq \theta \leq \pi$		$0 \leq \theta \leq \pi/2$		Percent-
E, eV	SM	HM	SM	HM	age[a]
1	1.06	0.93	1.06	0.93	77
3	3.00	3.14	2.11	2.32	99
4	3.14	3.83	1.87	1.96	99
7	1.95	2.76	1.16	1.11	86
10	1.11	2.18	0.53	0.67	73
15	0.60	1.06	0.29	0.29	83

[a] See footnote a, Table I.

In the first case, atom X is allowed to approach the molecule from all directions, whereas in the second it is allowed to approach only from those directions for which, at time $t = 0$, atom Z is more or less between atom X and atom Y. On applying the model to practical cases, this assumption enables us to distinguish between the two reactions

$$ZY + X \longrightarrow \begin{cases} ZX + Y \\ YX + Z \end{cases}$$

As mentioned earlier, the comparison is performed by calculating the trajectories according to each model when the same initial conditions are chosen for both. It should be noted that the "fertile" initial conditions (those for which the trajectories end in reactions) are not necessarily the same in the two models; the percentage which does happen to be the same in both models was calculated, and the results are shown in column 5 of each table. It is seen that on the whole, in a high percentage of cases, those trajectories that lead to reactions in one model will also do so in the other model.

Considering the results summarized in the tables (particularly columns 3 and 4), it is seen that the fit between the two models is satisfactory. This fit was achieved by the adjustment of one parameter only ($r_{0x} = r_{0y}$). All the other parameters used in HM were derived, as described, from SM.

Further details on the comparison between SM and HM can be derived from Figures 3–11, which represent the internal and translational energy distributions of the newly formed molecules. We notice that as a rule the newly formed molecules are more excited (internally and translationally) in SM than in HM, which means that in HM the atom Y carries away more energy from the system ZX than it does in SM. This phenomenon is rather general, almost independent of the initial energy of the projectile, and means that the three-body interaction in SM is not a chain of successive pure two-body interactions.

Discussion of the Results

In this work reactive cross sections were computed using (1) an energy-dependent hard model, and (2) the soft model due to Karplus and Raff. The calculations were performed almost for the entire reactive zone (namely, for energies above the thermal region) and for three different sets of masses. The results enable us to evaluate the importance of the different parameters defining the potential energy surfaces applied in both models.

In ref 1 it was already recognized that in order to obtain the correct dependence of the total reactive cross section on the energy, it was necessary to introduce an energy dependence of ρ_{xy} (defined as the radius of the hard-sphere potential $V_{xy}(r_{xy})$ governing the interaction between X and Y). This was further confirmed in the present work. However, it was shown that an energy dependence such as that suggested in ref 1, where the dependence on the impact parameter was ignored, would not always yield the desired results. When $m_z \ll m_x$, m_y, the reactive cross sections according to HM were much smaller than those according to SM; this discrepancy was resolved by extracting ρ_{xy} from eq 26a instead of 26b, which yielded larger cross sections for collision between X and Y, and consequently larger reactive cross sections. In this connection we should also mention the other modification introduced here, namely, the adjustment of the relative position of Y at time $t = 0$. This was found to be necessary particularly when $m_z \ll m_x$, and when the energy was high (>10 eV). The fact that these

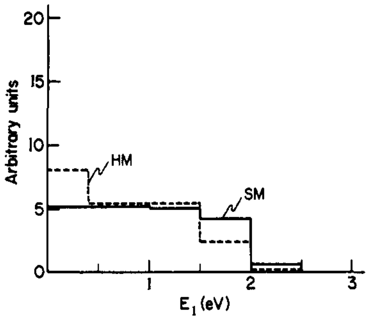

Figure 3. Translational energy distribution of the newly formed molecule ZX for the case $m_x = m_y = 10$ mu, $m_z = 1$ mu; $E = 3$ eV.

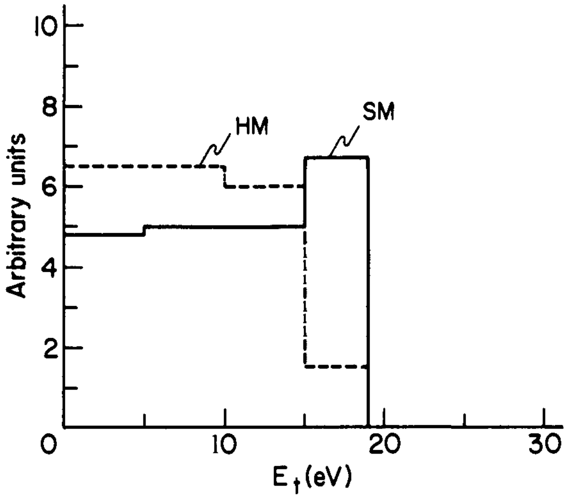

Figure 4. The same as Figure 3, but with $m_x = m_y = 10$ mu, $m_z = 1$ mu; $E = 20$ eV.

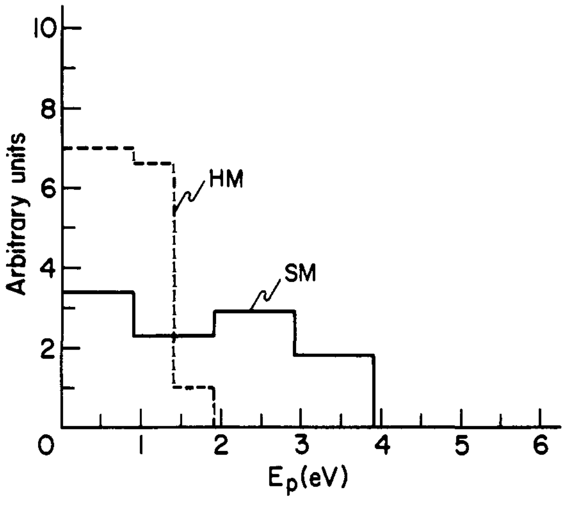

Figure 5. Internal energy distribution of the newly formed molecule ZX, for the case $m_x = m_y = 10$ mu, $m_z = 1$ mu; $E = 20$ eV.

modifications of the two-body potential between X and Y had to be added to the HM in order to get a fit with the SM indicates that under the above mass and energy conditions the reactive cross sections are rather sensitive to the potential.

In the SM, therefore, we conclude that the repulsion term in the Blais–Bunker potential is decisive, and any change in it will lead to different results. The sensitivity becomes more pronounced the higher the energy of X and the larger the mass of X compared with that of Z.

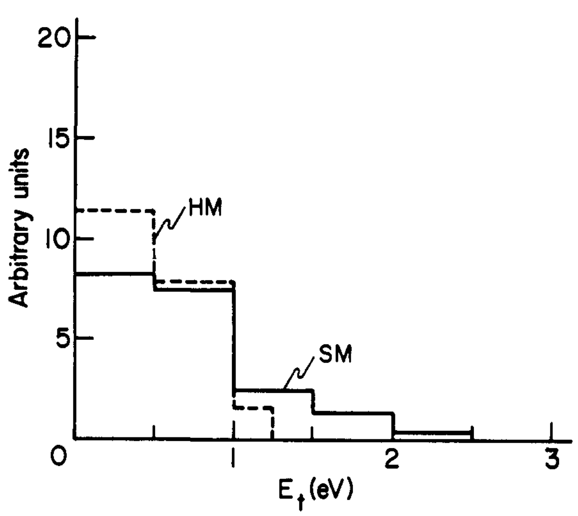

Figure 6. Translational energy distribution of the newly formed molecule ZX, for the case $m_x = m_y = m_z = 1$ mu; $E = 3$ eV.

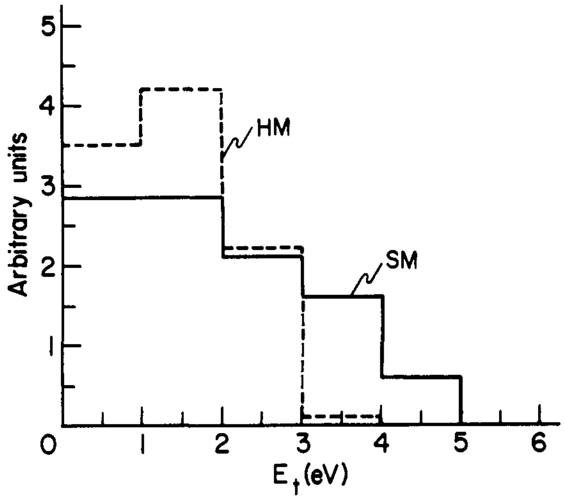

Figure 7. The same as Figure 6, but with $m_x = m_y = m_z = 1$ mu; $E = 10$ eV.

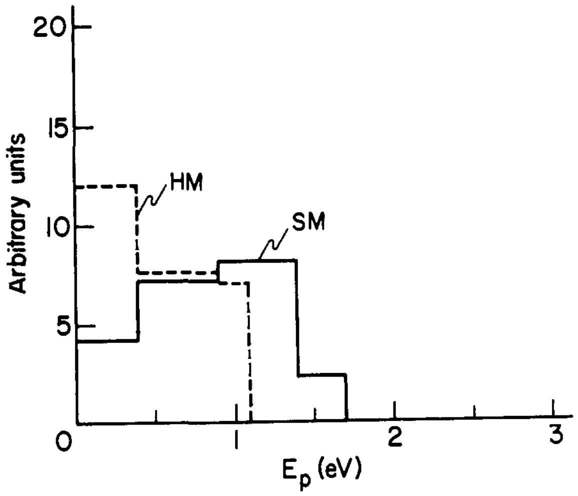

Figure 8. Internal energy distribution of the newly formed molecule ZX, for the case $m_x = m_y = m_z = 1$ mu; $E = 3$ eV.

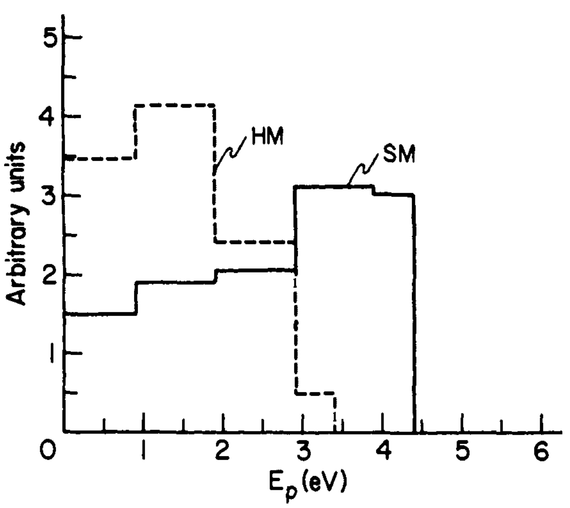

Figure 9. The same as Figure 8, but with $m_x = m_y = m_z = 1$ mu; $E = 10$ eV.

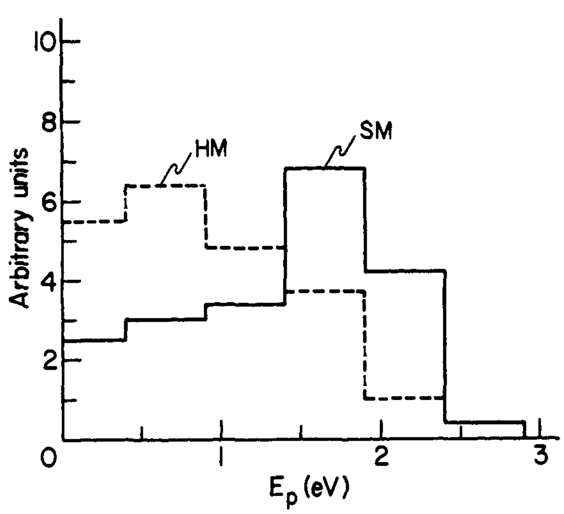

Figure 10. The same as Figure 8, but with $m_x = m_y = 1$ mu, $m_z = 10$ mu; $E = 3$ eV.

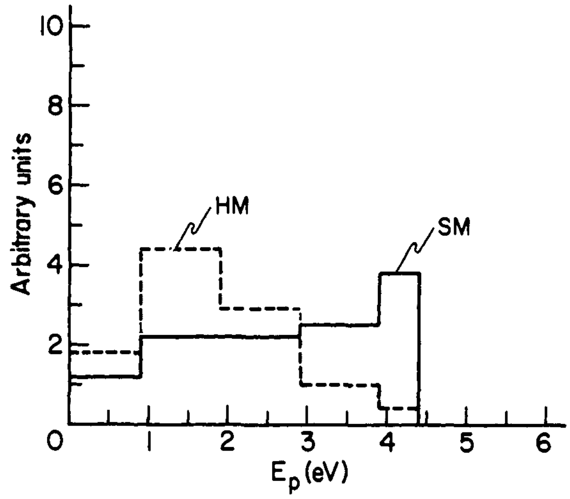

Figure 11. The same Figure 8, but with $m_x = m_y = 1$ mu, $m_z = 10$ mu; $E = 7$ eV.

In the present work we assumed R_x and R_y, the radii of the potential wells which replaced the Morse potential in the Blais–Bunker potential, to be energy dependent, even though it seemed that except for certain cases satisfactory results could be obtained without doing so. In general, using small radii of attraction (of about the bond length) gave good results as long as m_z was not too large compared with m_x. However, for $m_z \gg m_x$, and for energies higher than E_{th} (>10 eV), a fixed small radius of attraction led to results which were too high. The use of relatively large radii of attraction reduced the total reactive cross sections by preventing the formation of molecules with internal energies higher than the binding energy. The agreement between the results of the SM and HM that could be achieved without making R_x and R_y energy dependent indicates the relatively low sensitivity to the shape of the attractive part of the (Morse) potential, as long as m_z is not too large compared with m_x. If, however, $m_z \gg m_x$, one finds that the detailed structure of the attractive part of the potential will indeed influence the results.

Concerning the inner repulsive part of the Morse potential, it was found that ρ_y, the radius of repulsion for that part of the potential, does not have to be made energy dependent except at very high energies (~100 eV). This shows that this part of the potential has in fact no influence on the final results.

To sum up, the good fit obtained between the total reactive cross sections calculated by the SM and HM models, for energies less than 10 eV (but above the thermal region), indicates an insensitivity of the cross sections to the details of the potential energy surface.[16] Thus it is impossible to check the models by comparison with experiments in this energy region. Above 10 eV, however, the results given by the two models diverge for certain mass conditions, and here experiments are called for. By going from one set of masses to another, information can be derived on different parts of the potential. For example, for $m_x \ll m_z$, more information can be derived on the attractive portion of the (Morse) potential, whereas for $m_x \gg m_z$, more information can be derived on the direct interaction between X and the entire molecule, *i.e.*, on the repulsive part.

The situation is completely different if differential cross sections are considered. Since in this case the results derived from HM are always in disagreement with those obtained using SM, we may conclude that cross molecular beam type experiments where various kinds of differential cross sections are measured could give a good indication on what type of potential is really governing the interaction in the considered energy range.

Acknowledgments. The authors wish to express their thanks to Professor M. Karplus of Harvard University for helpful discussions on the different aspects of the problem. We would also like to acknowledge the cooperation of Mr. Z. B. Alfassi who programmed one of the computer programs used in this work.

---

(16) This conclusion was criticized by a referee, who pointed out that it contradicts other recent studies [*cf.* P. J. Kuntz, E. M. Memeth, J. C. Polanyi, and W. H. Wong, *J. Chem. Phys.*, **52**, 4654 (1970)]. Consequently we decided to study this point in greater detail, and the results will be reported in a subsequent paper.